Ferromagnetoelastic Resonance in Thin Films. II. Application to Nickel*

T. Kobayashi,† R. C. Barker, and A. Yelon‡
Department of Engineering and Applied Science, Yale University, New Haven, Connecticut 06520
(Received 10 May 1072)

In Paper I we presented a formal treatment of ferromagnetoelastic resonance (FMER) in thin films. In the present paper, this method is applied to the calculation of resonance lines of nickel at room temperature and at 25.92 GHz, a K-band frequency. It is shown that the FMER conditions are the following: (i) The film thickness nearly equals an odd-integral number of half-wavelengths of the elastic wave at the ferromagnetic-resonance frequency under the spin-unpinned and traction-free boundary conditions, or under the spin-pinned and traction-free boundary conditions; (ii) the film thickness nearly equals an even-integral number of half-wavelengths of the elastic wave under the spin-pinned and deformation-free boundary conditions. The thickness range over which the linewidth enhancement occurs is about 3% of the FMER thickness. The effect of the elastic damping on the linewidth enhancement is discussed. The angular dependence of the linewidth is examined in detail, along with the resonance-frequency shift and line shape. Finally, the relationship of the FMER problem to that of phonon generation is discussed briefly.

I. INTRODUCTION

In a previous paper[1] (hereafter referred to as I), a formal treatment of the solution of the coupled magnetoelastic equations of motion for obliquely magnetized thin films has been presented. Two methods of solution have been discussed. The first is exact within the framework of the quasistatic approximation (ferromagnetic insulator). It shows that magnetoelasticity has an appreciable effect on the resonance linewidth only in the special situation in which an elastic wave undergoes a thickness resonance at or near the ferromagnetic-resonance (FMR) frequency. This is also the condition for maximum phonon generation. We call this special case the ferromagnetoelastic resonance (FMER). The second method makes use of a self-consistent approximation based on the observation that strong coupling exists only between the resonant spin wave and the thickness-resonant elastic wave. The approximate method reduces the required computer time by a factor of 10 with a loss of less than 1% in the accuracy of the calculation of the power absorbed.

The approximate method, therefore, is convenient for calculating the magnetic and elastic responses of the coupled system over a wide range of magnetic and elastic material parameters and boundary conditions. Some calculations of the phonon generation under resonant and nonresonant conditions have already been reported.[2,3] The present paper treats the magnetic response of nickel at room temperature and at K-band frequency (but ignoring conductivity), with emphasis on the resonance line shape and linewidth near the FMER condition. As the results of the calculation are developed, they are described in terms of a model of a coupled pair of resonant circuits. Under many physically reasonable conditions, these circuits may be overcoupled.

While the influence of the frequency, field, and film thickness upon FMR has been considered for situations when the spin-wave and acoustical branches of the dispersion relation are near crossover,[4,5] the possibility of the acoustical-wave resonance seems not to have been examined until recently.[6] It is the purpose of this paper, therefore, to demonstrate that FMER should be observable in films and plates of magnetostrictive materials, and to anticipate the magnitude of the effect on the resonance line and the conditions under which it should be observed.

As the conditions for optimum generation of phonons by FMR are the same as the conditions for FMER,[2,3,7] the physical intuitive model presented here gives insight into this effect as well. Our calculations of phonon generation[2,3] appear to explain some of the apparent discrepancy between the wavelengths of the corresponding magnons and phonons in nickel and permalloy films[8–12] by showing that the unpinned, uniform-precession mode should be more efficient in generating phonons than the pinned mode. They have also shown that in maximizing the phonon power transmitted to a substrate, the acoustical-resonance condition is dominant. Thus, the substrate acoustical impedance should be severely mismatched rather than matched to the impedance of the ferromagnetic film. The existence of FMER modes, rather than magnetostatic modes, may account for oscillations with the field of the insertion loss in yttrium-iron garnet (YIG).[13] The possibility of FMER effects on the main resonance line suggests that the analysis of line shape in a properly designed experiment could yield the magnetoacoustic parameters (particularly the elastic damping), without the need for a direct measurement of the phonon intensity.

We begin here with the definition of the FMER

TABLE I. Physical constants.

ρ	c_{11}	c_{44}	B_1	B_2	M_0	A^a	$\gamma/2\pi$	$\lambda/2\pi^b$	$\omega_0/\lvert\gamma\rvert$
8.9 g/cm^3	2.461×10^{12} erg/cm^3	1.220×10^{12} erg/cm^3	7.63×10^{7} erg/cm^3	8.54×10^{7} erg/cm^3	485 G	0.8×10^{-6} erg/cm	-3.074×10^{6} Hz/Oe	3.75×10^{7} Hz	8432 Oe

[a] $2A/M_0 \equiv D = 3.3\times10^{-9}$ Oe cm^2.

[b] $\lambda/\gamma M_0 \equiv \eta = -2.515\times10^{-2}$.

frequency and thickness. A section on the calculation of FMER absorption lines, using the physical constants of Table I, follows. We discuss the effect of elastic damping, the thickness dependence of linewidth, the angular dependence of linewidth, and the resonance-frequency shift and line shape. Finally, we consider the physical significance of these results.

II. FMER FREQUENCY AND THICKNESS

A magnetoelastic system can be viewed as two coupled resonant systems, which can be driven magnetically or elastically. Let us suppose that these systems are uncoupled and undamped, and driven independently by some external drive source with variable frequency ω and consider their responses. In I, in treating the approximate method we showed that the resonant part of the magnetic system is represented by a uniform-precession mode (μ_1^0) and a spin wave (μ_1'). The dispersion curve corresponding to μ_1^0 lies along the ω axis ($k=0$). The dispersion relation corresponding to μ_1' is given by

$$Dk^2 + H_0 + 2\pi M_0 \sin^2\theta - [(2\pi M_0 \sin^2\theta)^2 + (\omega/\gamma)^2]^{1/2} = 0 \ . \quad (1)$$

For the spin-unpinned (SU) boundary condition, the magnetic response is described solely by μ_1^0, which has a resonance at

$$\omega = |\gamma|\,[H_0(H_0 + 4\pi M_0 \sin^2\theta)]^{1/2} \ . \quad (2)$$

For the spin-pinned (SP) boundary condition, it is well known that the magnetic response has thickness resonances[14] when k, given by Eq. (1), equals $n\pi/L$, where n is any odd integer and L is the film thickness. If we solve Eq. (1) for ω with $k = n\pi/L$, we obtain the resonant frequency of the magnetic system:

$$\omega_n^m = |\gamma|\,\{[H_0 + D(n\pi/L)^2] \times [H_0 + 4\pi M_0 \sin^2\theta + D(n\pi/L)^2]\} \ . \quad (3)$$

Equation (3) includes Eq. (2) if we allow $n=0$ for the SU case. ω_n^m is shown in Fig. 1.

The dispersion relation of the elastic system is given by

$$ck^2 - \rho\omega^2 = 0 \ , \quad (4)$$

where $c = c_{11}$ for the longitudinal (L) elastic wave and $c = c_{44}$ for the transverse (T) elastic wave. For traction-free (TF) boundary conditions, the elastic response has thickness resonances when k equals $n\pi/L$ with n an odd integer, since the film surfaces serve as antinodes.[1] For deformation-free (DF) boundary conditions, the elastic system resonates when k equals $n\pi/L$ with n an even integer, since the surfaces act as nodes. Combining the two cases, we can write the resonance frequency of the elastic system as

$$\omega_n^p = (c/\rho)^{1/2}(n\pi/L) \ . \quad (5)$$

ω_n^p, the nth resonance of the phonon system, is shown in Fig. 1.

If we take damping into account, each resonance has a finite linewidth. If we also "turn on" the magnetoelastic coupling, the two systems are no longer independent. Suppose the magnetic system is driven by an external rf field with variable ω. Then, for a given ω (see Fig. 1), the magnetic response has k_m and k_p components together with the $k=0$ component driven directly by the external rf field. The elastic response also has k_p and k_m components. The amplitude (and phase) of each

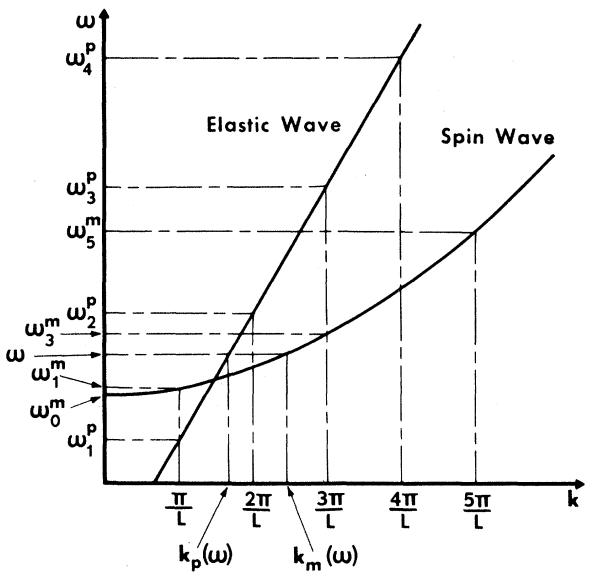

FIG. 1. Thickness resonance frequencies of the magnons and phonons for a given thickness L are labeled ω_n^m and ω_n^p, respectively, n corresponding to a mode number. Wave numbers for the magnons and phonons for an arbitrary frequency ω are labeled k_m and k_p, respectively.

component is determined by boundary conditions.

Since the resonant frequency of the elastic system (and of the magnetic system for the SP case) is a function of the thickness L, ω^p can be tuned to ω^m by varying L. When ω^p and ω^m coincide, the situation is what is called the magnetoelastic resonance. In the present analysis we consider only the magnetoelastic resonances in which the main resonance modes of the magnetic system ($n=0$ for the SU case and $n=1$ for the SP case) are involved. This we have called the ferromagnetoelastic resonance.

We now look for the frequency (ω_R) and thickness (L_R) at which the FMER occurs. For the SU-TF case, the resonant frequency of the (uncoupled) magnetic system is ω_0 and is independent of L. Hence, $\omega_R=\omega_0$. L_R must then be the thickness which tunes ω_n^p (n odd) to ω_0. Thus, $L_R=n\pi/k_p(\omega_0)$ (n odd). The wave configurations for $n=1$ and $n=3$ are schematically illustrated in Figs. 2(a) and 2(b). For the SP-TF case, both ω_1^m and ω_n^p (n odd) depend on L (see Fig. 1). The wave configurations for $n=1$ and $n=3$ are shown in Figs. 2(c) and 2(d). Clearly, the phonon wave number is n times the magnon wave number. Thus ω_R is the frequency at which $k_p=nk_m$ (n odd) is satisfied, and $L_R=\pi/k_m(\omega_R)$, where k_m is found from Eq. (1). Note that for $n=1$, $\omega_R=\omega_{cr}$, the crossover frequency, and $L_R=\pi/k_{cr}$. For the SP-DF case, ω_1^m and ω_n^p (n even) are also L dependent. The wave configurations for $n=2$ and $n=4$ are depicted in Figs. 2(e) and 2(f). It is apparent that ω_R is the frequency at which $k_p=nk_m$ (n even) is satisfied, and that $L_R=\pi/k_m(\omega_R)$. In the SU-DF case, only the uniform precession is excited, and there is no FMER.[1]

If the elastic system is viewed from the magnetic system, it corresponds to an extra loss. Under the FMER conditions, therefore, the resonance absorption line (of the magnetic system) is expected to broaden. The amount of broadening depends on three factors: the ratio of the elastic-resonance linewidth to the magnetic-resonance linewidth, which is determined by the ratio of the elastic damping to the magnetic damping, the relative position of the elastic-resonance frequency and the magnetic-resonance frequency, which is determined by the thickness, and the intensity of the elastic response, which is determined by the magnetoelastic coupling.

In Sec. III we present numerical calculations of the FMER absorption line and investigate its dependence on the parameters mentioned above.

III. FMER ABSORPTION LINES

A. Effect of Elastic Damping

As mentioned in Sec. II, the line broadening depends upon the ratio of the elastic damping to the magnetic damping. Let us define the quality factors of the magnetic and elastic systems, respectively, as

$$Q_m=\omega_0\tau_m=1/|\eta|\ ,$$
$$Q_p=\omega_0\tau_p=c'/2c''\ , \tag{6}$$

where τ_m is the phenomenological relaxation time of the $k=0$ magnon[15] and τ_p is that of phonons, and where the magnetic-damping constant $\eta=\lambda/\gamma M_0$, where λ is the Landau–Lifshitz (LL) damping parameter, and c' and c'' are the real (c_{11}' or c_{44}') and imaginary (c_{11}'' or c_{44}'') parts of the elastic constant.

For a given magnetoelastic coupling strength, if $Q_p \ll Q_m$, then the line broadening may be very small, since the elastic-resonance line is much broader than the magnetic-resonance line so that the elastic response does not change appreciably as ω is swept over the magnetic-resonance linewidth. On the other hand, if $Q_p \gg Q_m$, the effect is expected to be very large. The absorption peak may even split into two distinct peaks since the elastic response exhibits a narrow sharp resonance as ω is swept over the broader linewidth of the magnetic response. In the intermediate case, when Q_p is comparable with Q_m, the line broadening may or may not be appreciable, depending upon the other parameters.

Let us examine some typical absorption lines in

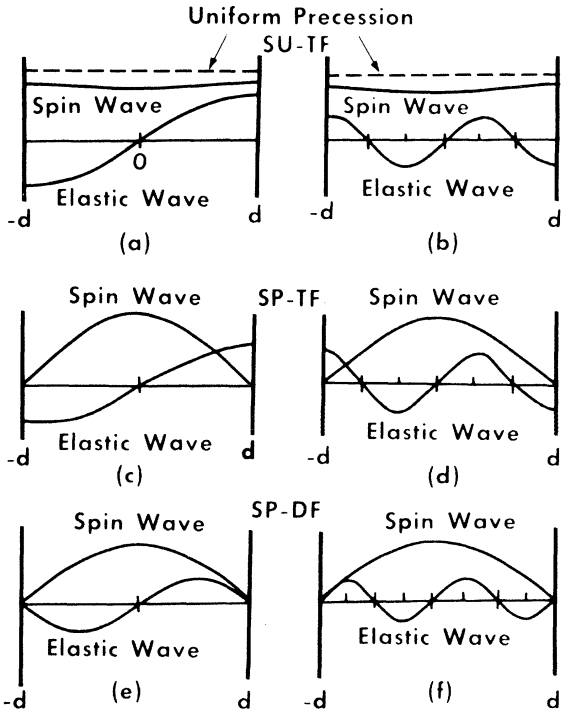

FIG. 2. Wave configurations under FMER conditions.

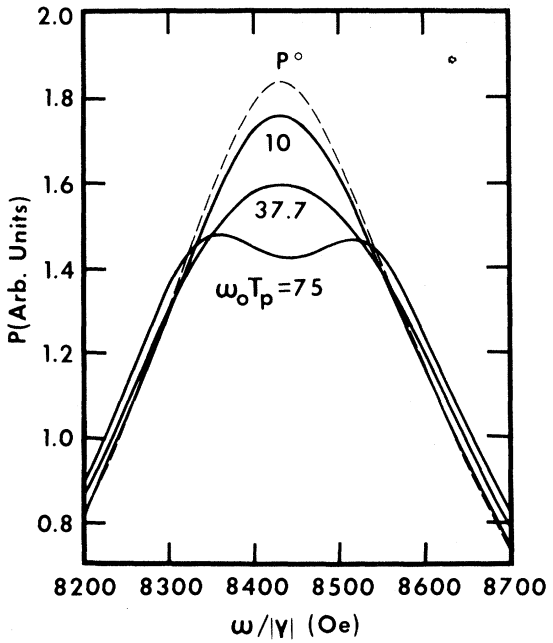

FIG. 3. Power-absorption lines for the SU-TF case with $\omega_0\tau_p$ as a parameter. The LE wave is in thickness resonance.

the SU-TF case with $\omega_0\tau_p$ taken as a parameter. Figure 3 shows the absorption lines for $\omega_0\tau_p = 10$, 37.7, and 75, which roughly correspond to the above three cases. The value of $\omega_0\tau_m$, corresponding to the value of the LL constant given in Table I, is 39.8. The thickness (1013 Å) satisfies the FMER condition ($\omega_1^p = \omega_0$) for the L elastic wave. 45° is the angle at which the L magnetoelastic coupling is strongest. The absorption line of the uncoupled system, which in this case is that of the uniform-precession mode, is also plotted for comparison.

Figure 3 shows that the absorption line for $\omega_0\tau_p = 10$ does not differ very much from that of the uncoupled case. For the case of $\omega_0\tau_p = 75$, it exhibits a double peak as mentioned above. The off-resonance absorption is greatly enhanced, as is usually the case with a resonant system coupled to another system with a higher Q. As a result, the linewidth is broadened appreciably. There is also line broadening for $\omega_0\tau_p = 37.7$.

It should be noted that the phonon relaxation time is not known for the frequencies of interest. Weber[4] and Seavey[5] estimated $\omega_0\tau_p = 37.7$ for permalloy at 60 GHz. Figure 4 shows how the resonance linewidth near the FMER condition changes as $\omega_0\tau_p$ is changed around 37.7. In the figure, 250 Oe corresponds to the linewidth for the uncoupled case (uniform-precession mode in the SU-TF case), which constitutes the background. The strong dependence of the linewidth enhancement on $\omega_0\tau_p$ implies that the value of $\omega_0\tau_p$ is critical to a quantitative estimate of the linewidth enhancement. We will, however, use $\omega_0\tau_p = 37.7$ for both L and T elastic waves in the present calculations. The sharp thickness resonance shown in Fig. 4 will be discussed below. A similar dependence of the linewidth enhancement on the elastic damping is also seen in the T-thickness-resonance case and in the SP-TF and SP-DF cases.

B. Thickness Dependence of Linewidth

Let us now consider what will happen to the linewidth when the thickness is varied around the FMER thickness (L_R). This has been shown, for the SU-TF case with the L elastic wave in thickness resonance ($n = 1$), in Fig. 4. We see from the figure that the linewidth abruptly increases from the background, for L within a narrow range about $L_R = 1013$ Å. If we define the FMER-thickness linewidth ΔL_R as the thickness range over which the frequency-linewidth enhancement occurs, then we find from Fig. 4 that ΔL_R is about 30 Å or $\Delta L_R/L_R = 0.03$. On the other hand, we find that the ratio of the linewidth to the resonance frequency $\Delta\omega_r/\omega_r$ of the uncoupled case is also about 0.03. This implies that the linewidth enhancement does not occur until the elastic-resonance frequency is tuned in approximately within the magnetic-resonance linewidth of the uncoupled case. Thus, we

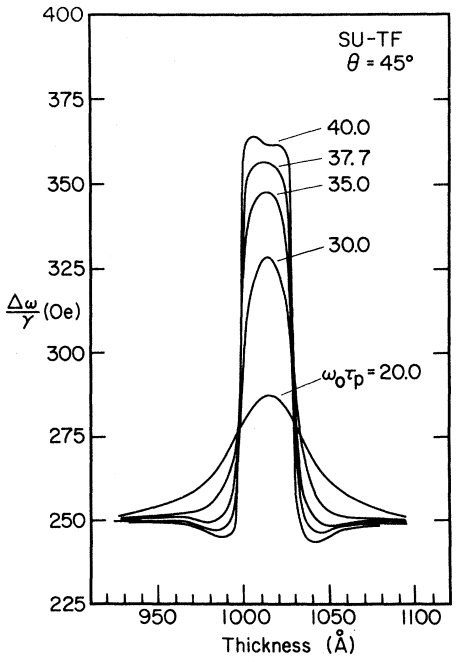

FIG. 4. Thickness dependence of $\Delta\omega/|\gamma|$ for the SU-TF case with $\omega_0\tau_p$ as a parameter. The LE wave is in thickness resonance.

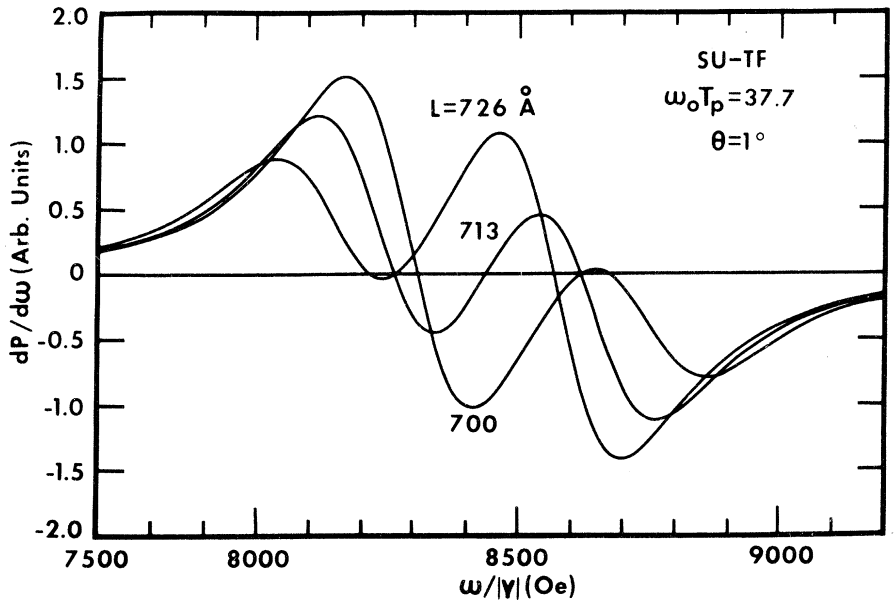

FIG. 5. Differential absorption lines for the SU-TF case with the TE wave in resonance. $L = 713$ Å corresponds to the FMER thickness for this case.

arrive at the following approximate formula for the FMER thickness linewidth:

$$\Delta L_R / L_R = \Delta \omega_r / \omega_r \ . \tag{7}$$

For the case of T thickness resonance, some absorption lines exhibit double peaks for $\omega \tau_p = 37.7$. This is shown in Fig. 5, in which the derivatives of three absorption lines ($dP/d\omega$) are plotted. This is due to the fact that the T magnetoelastic coupling is stronger than the L coupling for most angles. Equation (7), however, is still valid if the linewidth is defined as the frequency differences between the two largest extrema of $dP/d\omega$. According to this definition, $\Delta\omega/|\gamma| = 640$ Oe for $L = 713$ Å (which corresponds to L_R for this case), and $\Delta\omega/|\gamma| = 240$ Oe for $L = 700$ and 726 Å.

FMER also occurs for $n \geq 3$. We call this higher-order FMER. However, the linewidth enhancement decreases rapidly as n increases. We expect the intensity of the elastic response to fall off roughly as $1/n^2$ by analogy with the intensity fall-off of the spin-wave modes.[14] Hence, the linewidth

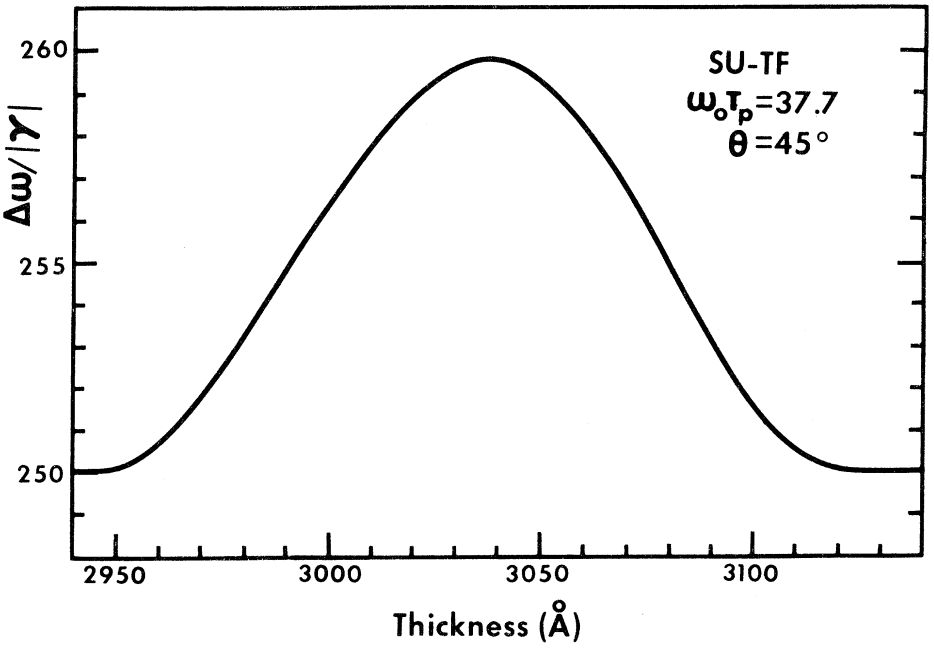

FIG. 6. Thickness dependence of $\Delta\omega/|\gamma|$ for the SU-TF case with the LE wave in resonance ($n = 3$).

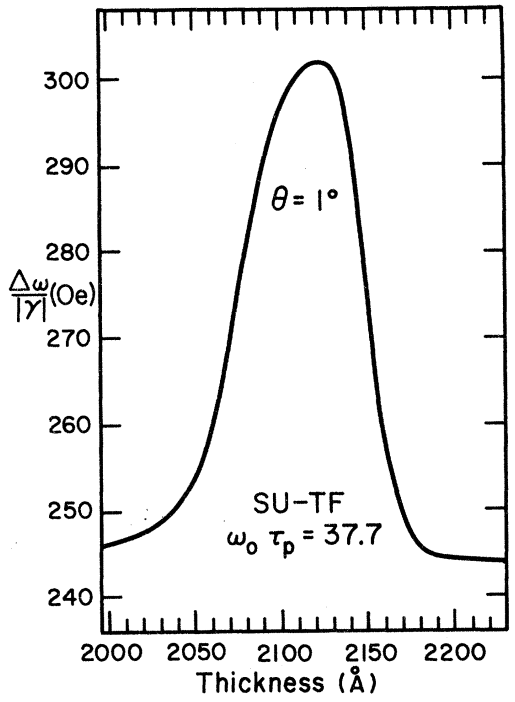

FIG. 7. Thickness dependence of $\Delta\omega/|\gamma|$ for the SU-TF case with the TE wave in resonance ($n=3$).

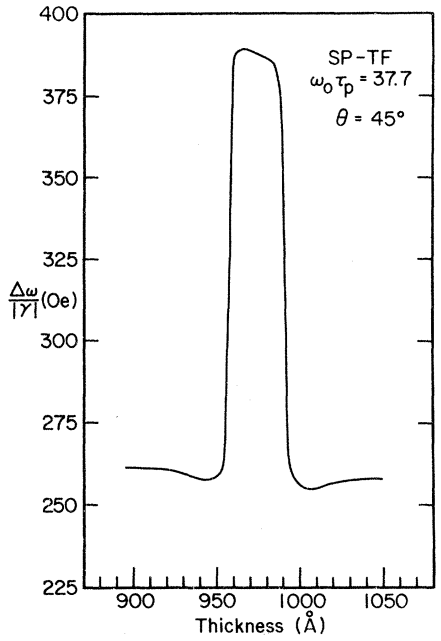

FIG. 8. Thickness dependence of $\Delta\omega/|\gamma|$ for the SP-TF case with the LE wave in resonance ($n=1$).

enhancement is also expected to fall off as $1/n^2$. Examples of higher-order FMER are shown in Figs. 6 and 7 for the SU-TF case with $n=3$. The wave configuration for this case corresponds to that of Fig. 2(b). Figure 6 shows the case with the L elastic wave in thickness resonance. The linewidth enhancement is 10 Oe, which is in agreement with the expected $1/3^2$ falloff. Figure 7 shows the case with the T elastic wave in thickness resonance. The falloff in this case is also about $1/3^2$ as expected (see the discussion in connection with Fig. 5). Note that ΔL_R is about three times that of the main ($n=1$) FMER as expected from Eq. (7).

Let us briefly discuss the situation for other

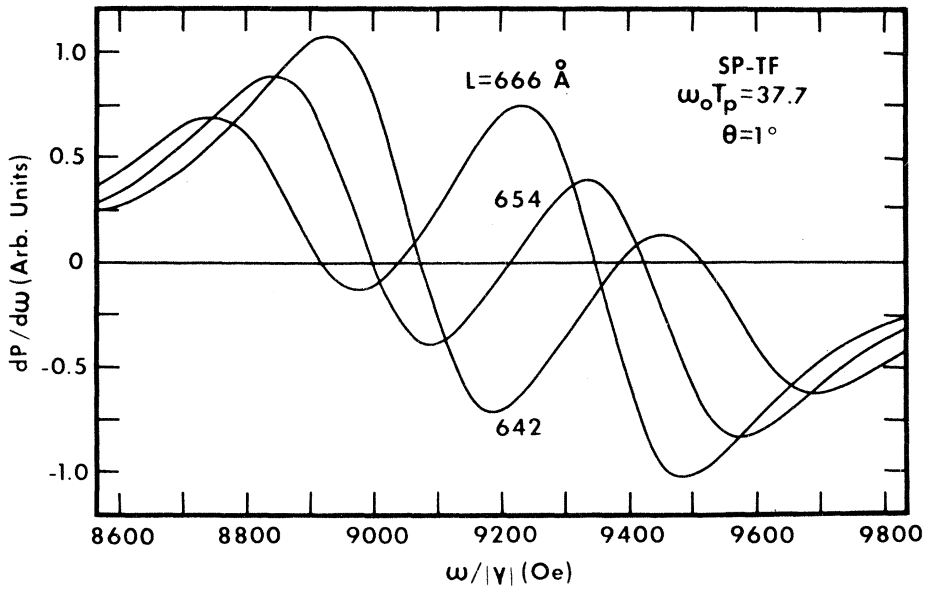

FIG. 9. Differential absorption lines for the SP-TF case with the TE wave in resonance. L = 654 Å corresponds to the FMER thickness for this case.

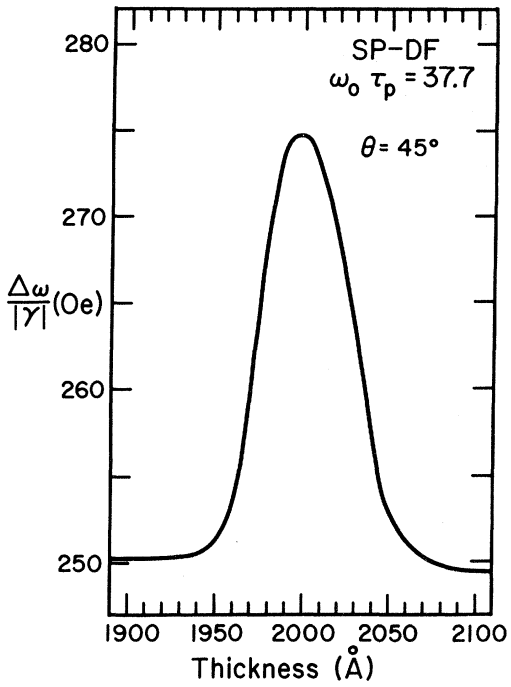

FIG. 10. Thickness dependence of $\Delta\omega/|\gamma|$ for the SP-DF case with the LE wave in resonance ($n=1$).

boundary conditions. Figure 8 shows the thickness dependence of the linewidth for the SP-TF case with the L elastic wave in thickness resonance ($n=1$). The linewidth enhancement is slightly larger than that for the SU-TF case shown in Fig. 4. This is expected because the FMER occurs at the magnetoelastic crossover. Some absorption lines for the case of T thickness resonance under the SP-TF condition show double peaks similar to those under the SU-TF condition. Examples are shown in Fig. 9. $\Delta\omega/|\gamma| = 730$ Oe for $L = 654$ Å ($= L_R$) and $\Delta\omega/|\gamma| = 260$ Oe for $L = 642$ and 666Å.

According to the $1/n^2$ law discussed above, the linewidth enhancement for the SP-DF case is expected to be approximately $1/2^2$ smaller than for the TF case, since L_R for the DF case contains a full wavelength of the elastic wave [see Fig. 2(e)]. Thickness dependences of the linewidth for the cases with the L elastic wave and the T elastic wave in thickness resonance are shown in Figs. 10 and 11. Comparison between Figs. 8 and 10 confirms the above estimate, although this estimate is somewhat crude because the elastic boundary conditions are not the same for the two cases.

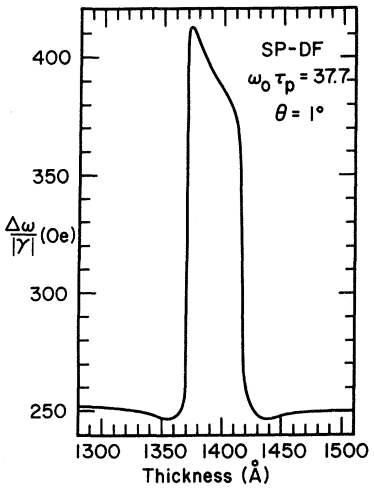

FIG. 11. Thickness dependence of $\Delta\omega/|\gamma|$ for the SP-DF case with the TE wave in resonance ($n=1$).

C. Angular Dependence of Linewidth

The angular dependence of the linewidth is almost solely characterized by the magnetoelastic coupling functions $f_L(\theta)$ and $f_T(\theta)$ which are defined, respectively, in Eqs. (42) and (57) of I. These functions are plotted against θ in Fig. 12. As seen from the figure, $f_L(\theta)$ is largest at about $\theta = 45°$ and vanishes at $\theta = 0$ and 90°, and $f_T(\theta)$ is largest at $\theta = 0$ and has a minimum at about 55°.

In Fig. 13 we show the angular dependence of the linewidth for the SU-TF case at three thicknesses for which three kinds of FMER occur. Curve L_1 is for the case of the first-order ($n=1$) FMER for the L elastic wave. Note the similarity between the curves of L_1 and of $f_L(\theta)$. The small departure from the exact proportionality is due to the angular dependence of the background (uniform-precession) linewidth, which is also plotted in Fig. 13. Curve T_1 is for the case of the first-order FMER for the

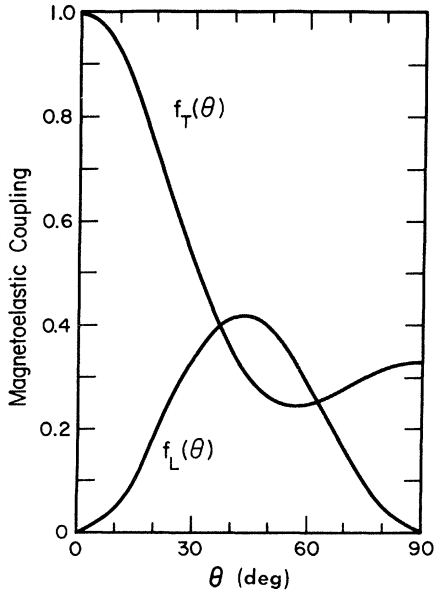

FIG. 12. Angular variations of the magnetoelastic coupling functions.

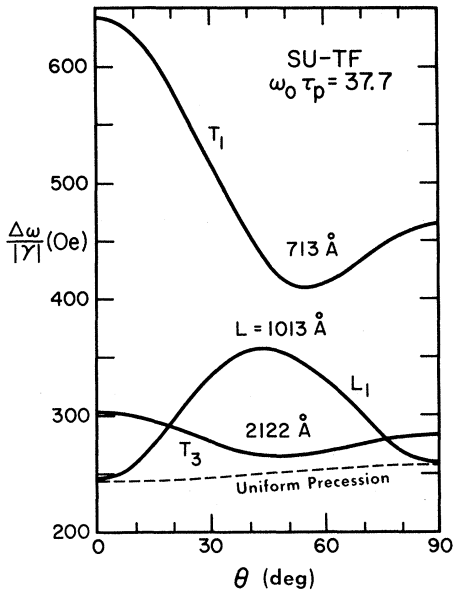

FIG. 13. Angular dependence of $\Delta\omega/|\gamma|$ for the SU-TF case at three thicknesses for which three kinds of FMER occur.

T elastic wave. Note again the similarity between the curves of T_1 and of $f_T(\theta)$. That $f_L(\theta)$ and $f_T(\theta)$ cross, while curves L_1 and T_1 do not, is mainly due to the fact that B_2^2 is some 25% larger than B_1^2,[16] where B_1 and B_2 are the L and T magnetoelastic constants, respectively. Curve T_3 is for the case of the third-order ($n=3$) FMER for the T elastic wave. Note that the approximately $1/3^2$ falloff is present for all angles. The similarity between the curves T_3 and $f_T(\theta)$ could be more easily seen if curve T_3 were drawn on a larger scale. Linewidths for the SP-TF and SP-DF cases show similar angular dependence.

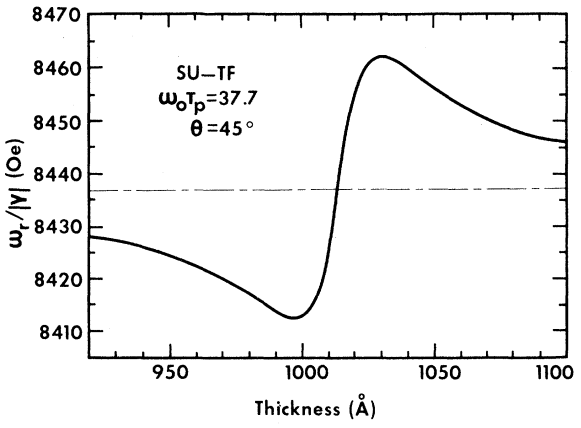

FIG. 14. Thickness dependence of the resonance frequency for the SU-TF case with the LE wave in resonance.

D. Resonance Frequency and Line Shape

In the absence of magnetoelastic coupling, the resonance frequency is obtained from Eq. (3):

$$\omega_r/|\gamma| = \{\beta[H_0 + D(n\pi/L)^2] \times [H_0 + 4\pi M_0 \sin^2\theta + D(n\pi/L)^2]\}^{1/2}, \quad (8)$$

where $n=0$ for the SU case and $n=1$ for the SP case. Note that $\beta = 1+\eta^2$ has been introduced in Eq. (8) to take account of the frequency shift due to the LL damping.[1,17]

In general, the magnetoelastic coupling also shifts the resonance frequency. However, if the elastic thickness resonance frequency ω^p is tuned exactly on ω_r (i.e., $L=L_R$), the shift disappears. If L is slightly increased from L_R, ω^p is tuned slightly lower than ω_r so that it pulls down the absorption line around ω^p and pushes the absorption peak slightly up to the higher side of ω_r. Hence, the resonance frequency shifts up. At some value of L, which turns out to be $L_R + \frac{1}{2}\Delta L_R$, the frequency shift reaches a maximum and comes back asymptotically to ω_r as L is further increased. If L is decreased from L_R, the situation is, of course, reversed and the frequency shifts symmetrically downward.

In Fig. 14 we have plotted $\omega_r/|\gamma|$ vs L for the SU-TF case with the L elastic wave in resonance. The thickness dependence of $\omega_r/|\gamma|$ for the SP-TF case with the L elastic wave in resonance is plotted in Fig. 15. Note that the resonance frequency of the uncoupled system is itself thickness

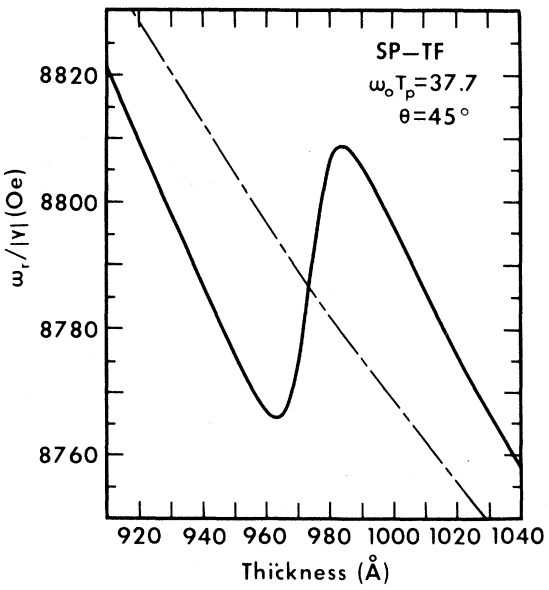

FIG. 15. Thickness dependence of the resonance frequency for the SP-TF case with LE wave in resonance.

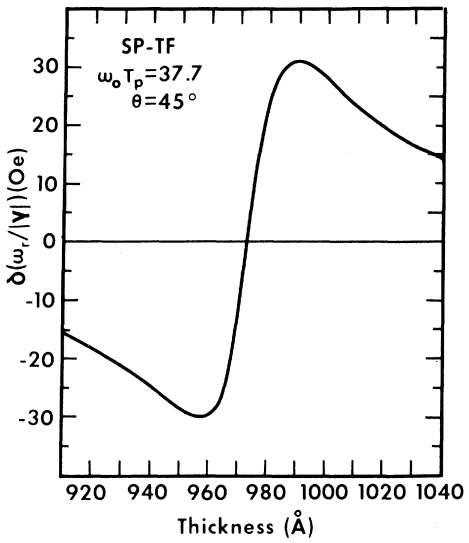

FIG. 16. Resonance-frequency shift as a function of thickness for the SP-TF case with the LE wave in resonance.

dependent for the SP case. If the frequency shift from $\omega_r/|\gamma|$ of the uncoupled system is plotted, as in Fig. 16, a curve similar to that of Fig. 14 is obtained. If one knows, for a given thickness, the resonance frequency shift $\delta(\omega_r/|\gamma|)$ at an angle $\theta = \theta'$, then $\delta(\omega_r/|\gamma|)$ at any angle θ can be obtained simply by

$$\delta\left(\frac{\omega_r}{|\gamma|}\right)_\theta = \left(\frac{f(\theta)}{f(\theta')}\right) \delta\left(\frac{\omega_r}{|\gamma|}\right)_{\theta=\theta'}, \tag{9}$$

where $f(\theta)$ is the magnetoelastic coupling function plotted in Fig. 12.

If an absorption line has a double peak, as in the case of the T thickness resonance under the SU-TF or the SP-TF condition, the resonance frequency is not uniquely determined. Examples of such lines are shown in Figs. 5 and 9. If either τ_p or the magnetoelastic coupling is decreased, the double peak gradually disappears and a unique resonance frequency is obtained. It is interesting to see how the double peak of the $L = 713$-Å curve shown in Fig. 5 disappears as θ is increased. This is illustrated in Fig. 17.

Line shape is closely related to frequency shift. Typical derivative line shapes are shown in Fig. 18. If $L = L_R$, then the thickness resonance merely broadens the linewidth and does not change the symmetry of the line. The symmetry is greatly distorted as the FMER is tuned off. As a measure of asymmetry, plotted against L in Fig. 19 is the ratio of two extrema of the $dP/d\omega$ curves, of which three curves have been sampled in Fig. 18. We note that the thickness difference between the two turning points again coincides with ΔL_R. A small deviation of the asymptote from unity (perfect symmetry) is due to the slight asymmetry of the uniform-precession resonance line at $\theta = 45°$.

Finally, it should be noted that the resonance-frequency shift shows a much broader thickness resonance compared with the resonance linewidth and line asymmetry. In other words, the thickness-dependence curve of the frequency shift (e.g., Fig. 14) has longer tails than those of the line asymmetry (Fig. 19) and of the linewidth (e.g., in Fig. 4, imagine the derivative of the linewidth with respect to the thickness). This is responsible for the resonance-frequency difference between the exact and approximate calculations shown in Fig. 3 of I. For $L = 1000$ Å, the T elastic wave, which is far from thickness resonance and therefore very weakly excited, contributes slightly to shifting up the resonance frequency in the exact calculation.

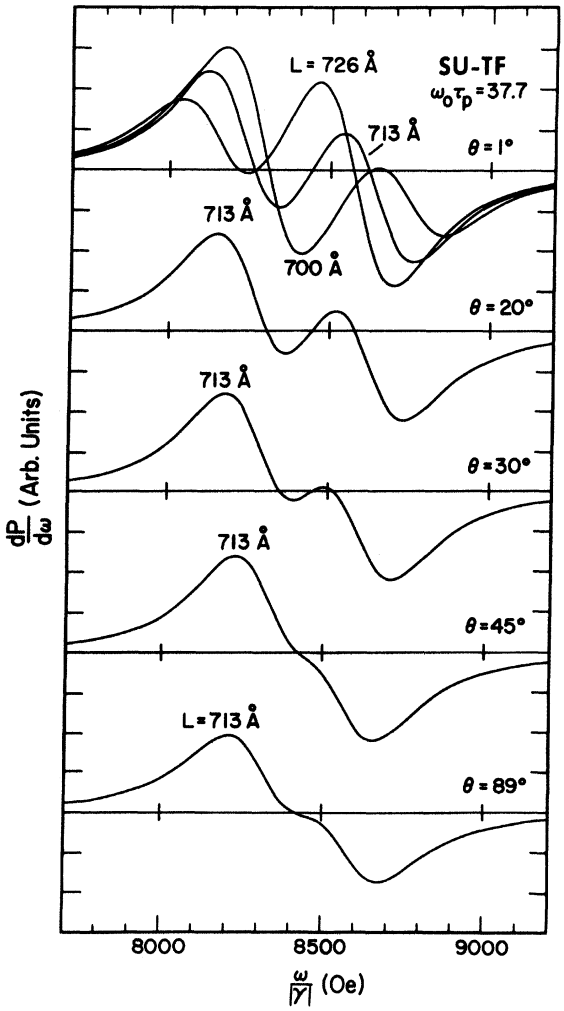

FIG. 17. Line-shape change with θ for the SU-TF case with the TE wave in resonance.

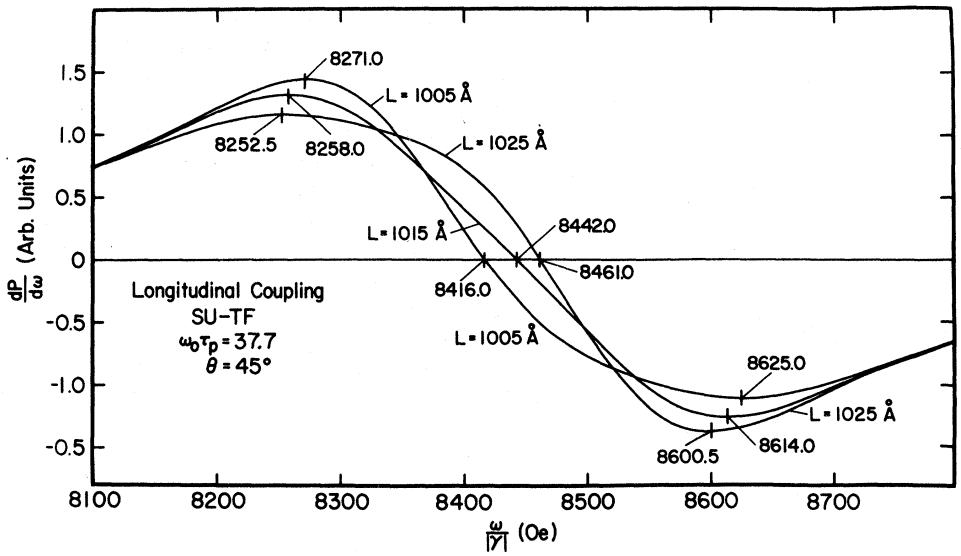

FIG. 18. Line shapes for the SU-TF case with the LE wave in resonance.

For $L = 800$ Å, the L elastic wave in the exact calculation contributes slightly to shifting down the resonance frequency.

IV. CONCLUSIONS

We have shown that magnetoelastic coupling, combined with isotropic magnetic and elastic damping, provides a mechanism for an appreciable anisotropy in the FMR linewidth of metal films. In I, we presented the exact and approximate methods for calculating this line broadening. The accuracy and range of validity of the approximate method were verified. In this paper we have applied the approximate method to the calculation of resonance lines of nickel (with zero conductivity) for various cases of interest.

The results of our study may be summarized as follows: (i) Magnetoelasticity has an appreciable effect on the resonance linewidth in the cases where an elastic wave undergoes a thickness resonance at or near the FMR frequency. (This is called the FMER.) (ii) The FMER occurs when the film thickness L equals an odd-integral number (n) of half-wavelengths of the elastic wave at the FMR frequency for the SU-TF and SP-TF cases, when L equals an even-integral number (n) of half-wavelengths of the elastic wave at the FMR frequency for the SP-DF cases, when the SU-DF case merely reduces to the uniform-precession problem so that there is no magnetoelastic effect. (iii) The effect decreases rapidly as n is increased. (iv) The thickness range over which the effect is

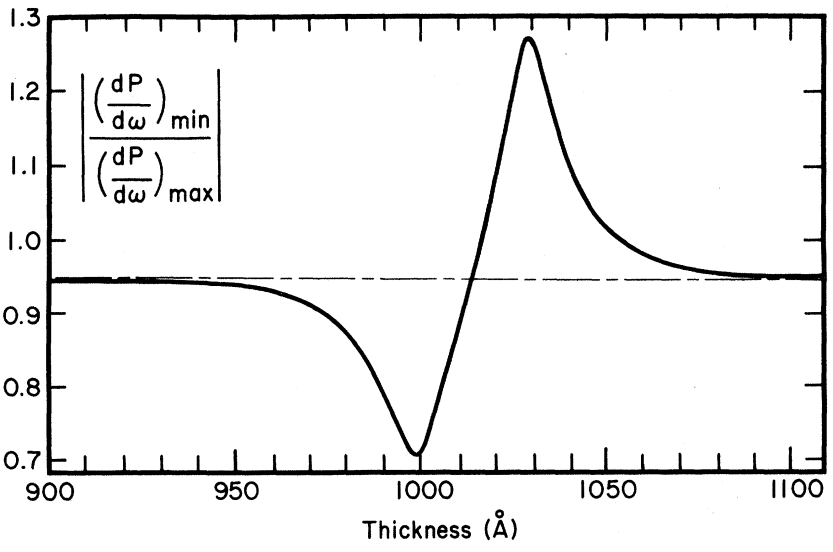

FIG. 19. Thickness dependence of the ratio of the two extrema of $dP/d\omega$ curves for the SU-TF case with the LE wave in resonance.

significant (FMER thickness linewidth ΔL_R) is approximately given by the formula

$$\Delta L_R/L_R = \Delta\omega_r/\omega_r ,$$

where L_R is the FMER thickness defined in (ii), and ω_r and $\Delta\omega_r$ are the resonance frequency and linewidth of the magnetic system without magnetoelastic coupling. (v) Under the FMER conditions the linewidth enhancement depends strongly upon the elastic damping and the angle θ between $\vec{M}_0$ and the film normal. (vi) If the elastic damping is comparable to the magnetic damping, the linewidth enhancement is as much as 50% at $\theta = 45°$ for the case of L thickness resonance and more than 100% at $\theta = 0$ for the case of T thickness resonance. (vii) The angular dependence of the linewidth enhancement is almost solely determined by that of the magnetoelastic coupling. For the L-thickness-resonance case the linewidth enhancement is maximum at $\theta = 45°$ and vanishes at $\theta = 0$ and 90°, and for the case of T thickness resonance it is maximum at $\theta = 0$, decreases as θ is increased, reaches a minimum at 55°, and increases slightly as θ is further increased to 90°. (viii) The resonance frequency coincides with that of the uncoupled case for $L = L_R$, shifts up as L is increased from L_R, reaches a maximum shift at $L = L_R + \frac{1}{2}\Delta L_R$, and asymptotically approaches the resonance frequency of the uncoupled case. If L is decreased from L_R, the resonance frequency shifts down symmetrically.

Previous workers in the field, not having considered the possibility that FMER might exist have not deliberately attempted to establish conditions in which it might be observed. Is there any evidence that it has been observed? Vittoria *et al.*[18] have reported a peak in the angular dependence of the FMR linewidth of single-crystal nickel platelets which closely resembles the expected angular dependence for the L elastic wave in thickness resonance under SU-TF conditions.[6] However, more recent experiments[19] have indicated strongly that while this peak is frequency dependent, it appears at film thicknesses that do not correspond to thickness resonance. Experiments to demonstrate the existence of FMER in films of a suitable thickness and with suitable acoustical boundary conditions are in progress.

An important practical consideration in such an experimental demonstration is the problem of film smoothness. In a real film the thickness varies from one place on the surface to another because of surface roughness. In some cases this may be only a few atomic layers, but is likely to be greater with most evaporated, sputtered, or electroplated films. The effect of the thickness variation is such that it broadens the effective thickness linewidth ΔL_R of the linewidth-vs-thickness curves of Fig. 4. In the real film, therefore, the effective thickness range over which the linewidth enhancement occurs may be considerably larger than the calculated one. However, the thickness variation also tends to smear out the linewidth-vs-thickness curves. Consequently, if the thickness variation is very large, the linewidth enhancement will be washed out unless the elastic damping is very small.

It therefore seems that the observability of the FMER depends critically on the magnitude of the elastic damping. As mentioned above, the elastic damping of single-crystal nickel is not known for frequencies higher than 200 MHz.[20] This is due to technical difficulties which arise in the conventional pulse-echo technique at high frequencies.[21] However, if FMER is observable, it will provide us with an excellent method for measuring the elastic damping in the appropriate frequency range.

Finally, using our formalism we can solve many other interesting problems as pointed out in I and in the Introduction. For example, suppose a magnetic film is attached to a nonmagnetic medium. In our formalism this corresponds to a finite-stress (finite-acoustic-impedance) condition at one surface, instead of the TF (zero-acoustic-impedance) or DF (infinite-acoustic-impedance) condition. We can easily calculate the effect of such a substrate on ferromagnetic resonance.[7,22] It is this case in which the nonmagnetic medium is, for example, a quartz transducer which is most closely related to the problem of phonon generation by thin-film ferromagnetic resonance, which has been treated elsewhere.[2,3] The same formalism we have described here and in I, and the physical picture described here have permitted the calculation of phonon power transmitted into the substrate under arbitrary spin pinning and acoustic-impedance boundary conditions. This had not been possible in previous work.[8–11]

---

*Supported in part by the National Science Foundation.

†Present address: Central Research Laboratory, Hitachi, Ltd., Kokubunji, Tokyo, Japan.

‡Present address: Department de Génie Physique, Ecole Polytechnique, 2500 Ave Marie Guyard, Montreal 250, Canada.

[1]T. Kobayashi, R. C. Barker, J. L. Bleustein, and A. Yelon, preceding paper, Phys. Rev. B 7, 3273 (1973).

[2]T. Kobayashi, R. C. Barker and A. Yelon, IEEE Trans. Magn. 7, 755 (1971).

[3]T. Kobayashi, R. C. Barber, and A. Yelon, IEEE Trans. Magn. 8, 382 (1972).

[4]R. Weber, Phys. Rev. **169**, 451 (1968).

[5]M. H. Seavey, Jr., Phys. Rev. **170**, 560 (1968).

[6]T. Kobayashi, R. C. Barker, and A. Yelon, J. Phys. (Paris) 32, 560 (1971).

[7]T. Kobayashi, R. C. Barker, and A. Yelon, Proceedings of the

Fifth International Colloquium on Magnetic Thin Films, Hakone, Japan, April, 1972 (unpublished), p. D5-1.
[8]H. E. Bömmel and K. Dransfeld, Phys. Rev. Lett. **3**, 83 (1959).
[9]M. Pomerantz, Phys. Rev. Lett. **7**, 312 (1961).
[10]M. F. Lewis, T. G. Phillips, and H. M. Rosenberg, Phys. Lett. **1**, 198 (1962).
[11]M. H. Seavey, Jr., IEEE Trans. Ultrason. Eng. **10**, 49 (1963); Proc. IEEE **53**, 1387 (1965).
[12]P. E. Wigen, W. I. Dobrov, and M. R. Shanabarger, Phys. Rev. 14, A1827 (1965).
[13]J. H. Collins, D. A. Wilson, and F. A. Pizzarello, J. Appl. Phys. **40**, 1201 (1969); J. H. Collins (private communication).
[14]C. Kittel, Phys. Rev. **110**, 1295 (1958).
[15]It is more appropriate to define $\omega_0\tau_m$ as $(1/|\eta|)\{[H_0(H_0+4\pi M_0\sin^2\theta)]^{1/2}/(H_0+2\pi M_0\sin^2\theta)\}$, for then $1/\tau_m$ is directly proportional to the frequency linewidth of the uniform-precession mode defined by Eq. (11) of I. For K-band frequencies, however, the term in the brackets does not deviate very much from unity (1 at $\theta=0$ and 0.94 at $\theta=90°$).
[16]Note that the dispersion relations contain the square of the magnetoelastic constant. See Eqs. (41) and (56) of I.
[17]G. V. Skrotskii and L. V. Kurbatov, in *Ferromagnetic Resonance*, edited by S. V. Vonsovskii (Pergamon, Oxford, England, 1966).
[18]C. Vittoria, R. C. Barker, and A. Yelon, Phys. Rev. Lett. **19**, 792 (1967).
[19]Y. J. Liu, R. C. Barker, and A. Yelon (unpublished data).
[20]S. Levy and R. Truell, Rev. Mod. Phys. **25**, 140 (1953).
[21]B. Luthi (private communication).
[22]T. Kobayashi, R. C. Barker, J. L. Bleustein, and A. Yelon, Letters Appl. Eng. Sci. (to be published).

PHYSICAL REVIEW B VOLUME 7, NUMBER 7 1 APRIL 1973

Monte Carlo Calculation of the Scaling Equation of State for the Classical Heisenberg Ferromagnet

K. Binder*
IBM Zurich Research Laboratory, 8803 *Rüschlikon, Switzerland*

H. Müller-Krumbhaar
*Physikdepartment E*14, *Technische Universität München, D* 8046 *Garching, West Germany*
(Received 5 September 1972)

Using a Monte Carlo procedure with a self-consistent-field boundary condition, the magnetization of a simple cubic classical Heisenberg ferromagnet with nearest-neighbor interactions only is calculated. For reduced temperatures and reduced fields in the range $0.02 \leq |T/T_c - 1|$, $H/J \leq 0.5$ the data of this computer experiment can be described in terms of the "effective" critical exponents $0.31 \leq \beta \leq 0.35$, $1.33 \leq \gamma \leq 1.39$, and $4.9 \leq \delta \leq 5.3$. Although the present data are not very close to the critical point they do obey the homogeneity requirement and determine the scaling function rather precisely. This function agrees very well with the scaling function for the face-centered-cubic classical Heisenberg magnet derived recently by Milošević and Stanley using high-temperature–series-expansion techniques. This agreement supports their hypothesis that neither critical exponents nor the scaling function depend on the lattice structure in the Heisenberg model.

I. INTRODUCTION

Considerable effort has been devoted to derive the critical properties of three-dimensional Heisenberg ferromagnets.[1–26] Most of this research uses high-temperature–series-expansion techniques,[27] which yield direct information about the exponents γ, ν, η, and α. Making use of the scaling assumptions[28] one can then draw more conclusions also about the exponents β and δ. A more direct result concerning β has been derived by Stephenson and Wood[17] in the case of an fcc classical Heisenberg lattice. Inverting the series for the free energy in a magnetic field[16] these authors find $\beta = 0.38 \pm 0.03$. The series for other lattices and other values of spin turned out to be too irregular to yield very precise results.[18]

More recently, other estimates for the critical exponents have been given using the Wilson $\epsilon = 4 - d$ expansion technique[24,25] and also using approximate renormalization-group recursion relations.[26] Apart from the values of critical exponents, temperatures, and amplitudes, one is also interested in the homogeneous function determining the scaling equation of state.[28–30] An important question is whether this function is independent of "irrelevant" features of the system (e.g., lattice structure or value of spin) as conjectured by the hypothesis of universality.[31,32] So far, this function has been calculated for the fcc lattice only in both the $S = \frac{1}{2}$ and $S = \infty$ cases by Milošević and Stanley.[23] For the bcc lattice the scaling function has been given only in the $S = \frac{1}{2}$ case,[23] and no scaling functions have been available for the simple cubic (sc) lattice. This scaling function has also been calculated using the renormalization-group techniques.[33] Another interesting question concerns the regime of validity of this asymptotic description in terms of critical